

1 **The crucial influence of trophic status on the relative requirement of nitrogen to**  
2 **phosphorus for phytoplankton growth**

3 Mengqi Jiang<sup>1\*</sup>, Shin-ichi Nakano<sup>1</sup>,

4 <sup>1</sup> Center for Ecological Research, Kyoto University, 520-2113 Shiga, Japan

5 \* Corresponding author

6 Email addresses: mqjiang@ecology.kyoto-u.ac.jp (M.J.), nakano@ecology.kyoto-  
7 u.ac.jp (S.N.)

8 **Keywords:** nitrogen; phosphorus; trophic status; phytoplankton; nitrogen-to-  
9 phosphorus ratio; limiting factor

10 **Send correspondence to:** [Mengqi Jiang]

11 [Center for Ecological Research, Kyoto University, 520-2113 Shiga, Japan, 080-5711-  
12 6059, mqjiang@ecology.kyoto-u.ac.jp]

13 **Authorship statement**

14 MJ conceived the study design, performed experiments, analysed data, and wrote the  
15 first draft of the manuscript; SN contributed to data analysis and manuscript writing.

16 Both authors contributed substantially to the manuscript and gave final approval for  
17 publication.

18

19 **Highlights**

- 20 1. The relative N:P requirement for growth was explored for eight phytoplankton  
21 species.
- 22 2. Trophic status is negatively related to the N:P ratio required for optimal growth.
- 23 3. Both N and P are important for phytoplankton growth in eutrophic waters.
- 24 4. Phytoplankton tend to require higher N relative to P under low-nutrient conditions.
- 25 5. The results contribute to the ongoing debate of N vs. P limitation in freshwaters.
- 26

27 **Abstract**

28 Clarifying the pattern of relative nitrogen (N)-to-phosphorus (P)  
29 requirements for phytoplankton growth is of great significance for eutrophication  
30 migration and management of aquatic systems. Relative N-to- P requirement for  
31 phytoplankton growth is considered an essential trait determining species dominance  
32 within ecosystems and explaining phytoplankton response to nutrient availability.  
33 These requirements vary with environmental trophic statuses, though this variation  
34 remains unclear. Here, we evaluated the relative N-to-P requirements under different  
35 absolute nutrient levels using previous and current experimental data on eight  
36 phytoplankton species (three studied by us and five extrapolated from the previous  
37 studies). Results showed that relative N-to-P requirements for phytoplankton growth  
38 decreased as absolute nutrient levels increased. Thus, N may be crucial for enhancing  
39 phytoplankton growth under low nutrient conditions, whereas P may be the primary  
40 limiting factor of phytoplankton growth under sufficient nutrient conditions. This  
41 result applies to single species as well as species assemblages, which are independent  
42 of species shifts occurring along water N:P gradients. The response observed in our  
43 large trophic status level gradient may help elucidate the relative importance of N and  
44 P reductions in mitigating the impact of eutrophication on ecosystems.

## 45 **1. Introduction**

46 Nitrogen (N) and phosphorus (P) are two key macronutrients utilized in the  
47 biochemical functions of phytoplankton and are the main nutrients limiting  
48 phytoplankton growth in aquatic ecosystems (Elser *et al.* 2007; Paerl 2009; Abell *et*  
49 *al.* 2010). The relative importance of the N-to-P supply (i.e., the supply N:P ratio) for  
50 phytoplankton growth remains an important subject in research on waterbodies with  
51 various trophic statuses, including research on controlling nuisance phytoplankton  
52 blooms in eutrophic waters (Lewis *et al.* 2011; Paerl *et al.* 2011; Paerl *et al.* 2016) and  
53 enhancing primary production (and thus enhancing zooplankton biomass and fish  
54 production) in oligotrophic waters (Budy *et al.* 1998; Reeder 2017). However, the  
55 relative importance of these two elements for phytoplankton growth remains  
56 controversial. P is generally considered the main factor responsible for controlling  
57 phytoplankton growth (Carpenter 2008; Schindler *et al.* 2008) largely because the  
58 nitrogen fixation of some cyanobacterial species can fulfill their N requirements  
59 (Smith 1990). Contrastingly, N limits phytoplankton growth during bloom conditions  
60 in some eutrophic lakes (Chaffin *et al.* 2013). Accordingly, a dual nutrient control (N  
61 & P) strategy is considered more effective in controlling phytoplankton growth than  
62 either nutrient alone (Elser *et al.* 2007; Lewis *et al.* 2011; Paerl *et al.* 2016).  
63 Regardless, related studies have mainly focused on the relative N:P ratios and have  
64 seldom mentioned the influence of absolute nutrient levels, which vary greatly. As P  
65 accumulates faster than N in freshwaters exposed to anthropogenic impact, the

66 relationship between total nitrogen (TN) and total phosphorus (TP) is relevant to the  
67 trophic status of a waterbody, that is, high TN:TP ratios in oligotrophic waters and  
68 low TN:TP ratios in eutrophic waters (Downing & McCauley 1992; Yan *et al* 2016).  
69 However, absolute nutrient concentrations may have a greater impact on  
70 phytoplankton growth than relative nutrient ratios because phytoplankton tend to be  
71 insensitive to resource stoichiometry during their fast-growing phase (Klausmeier *et*  
72 *al.* 2004; Hilebrand *et al.* 2013; Yang *et al.* 2020). Accordingly, if absolute nutrient  
73 concentrations are not considered, discussions regarding N:P ratios become largely  
74 inaccurate. Therefore, establishing situations where various N:P ratios with different  
75 nutrient levels is a prerequisite for evaluating the relative importance of N:P ratios for  
76 phytoplankton growth.

77 Most studies on relative N:P requirements are based on observations of how  
78 phytoplankton respond to various supply N:P ratios (Liu & Vyverman 2015; Rasdi &  
79 Qin 2015; Thrane *et al.* 2016, 2017; Kelly *et al.* 2021). However, the importance of  
80 trophic status cannot be reflected by a single supply N:P ratio series. Specifically,  
81 phytoplankton biomass would increase with the increase in supply N:P ratio when N  
82 was limiting, and decrease with the increase in supply N:P ratio when P was limiting.  
83 A peak of phytoplankton biomass could be achieved at the supply N:P ratio where N  
84 and P are co-limiting, which has been termed the “optimal supply N:P ratio” (the red  
85 line in Fig. 1a and b) (Sperfeld *et al.* 2012; Sperfeld *et al.* 2016; Tilman 1980). The  
86 optimal supply N:P ratio is a definitive value derived from a gradient of supply N:P

87 ratios and an indicator for assessing the relative importance of N-to-P requirements  
88 (Thrane *et al.* 2016, 2017). However, the definitive optimal supply value has various  
89 possibilities. For example, if a nutrient supply of 16  $\mu\text{mol N L}^{-1}$  and 1  $\mu\text{mol P L}^{-1}$  was  
90 calculated as the optimal supply N:P ratio for the growth of a certain phytoplankton  
91 species, we cannot easily generalize that 16 is the optimal supply N:P ratio in any  
92 environmental condition. Although the nutrient supply of 16  $\mu\text{mol N L}^{-1}$  and 1  $\mu\text{mol P}$   
93  $\text{L}^{-1}$  was optimal in a specific series of N:P ratios, we cannot tell whether a nutrient  
94 combination of 32  $\mu\text{mol N L}^{-1}$  and 2  $\mu\text{mol P L}^{-1}$  or 8  $\mu\text{mol N L}^{-1}$  and 0.5  $\mu\text{mol P L}^{-1}$   
95 would also be optimal among different supply N:P ratio gradients, despite having a  
96 ratio of 16. That is, the relative N:P requirement for phytoplankton may not be  
97 equivalent for higher or lower trophic statuses.

98       A definite optimal N:P ratio indicates that the relative importance of N-to-P  
99 requirement for phytoplankton growth remains unchanged under different trophic  
100 statuses (red line in Fig. 1a and b). Yet, N and P limitations affect phytoplankton cell  
101 physiology in significantly different ways. Protein is the largest N-containing  
102 component in phytoplankton cells, whereas P is distributed among phospholipids,  
103 adenosine triphosphate, and nucleic acids, especially ribosomal ribonucleic acid  
104 (rRNA) (Geider & La Roche 2002). N limitation hampers phytoplankton  
105 photosynthesis by causing large declines in the availability of photosynthetic  
106 pigments and Rubisco pools (Geider *et al.* 1993; Geider *et al.* 1998). Meanwhile, P  
107 limitation greatly suppresses phytoplankton growth because of the large investment of

108 P in rRNAs and the growth dependence of protein synthesis driven by P-rich  
109 ribosomes (Sterner & Elser 2002; Loladze & Elser 2011). Owing to these differences  
110 in the physiological functions of N and P, the relative importance of N:P requirements  
111 for phytoplankton growth may vary temporally among different environmental  
112 conditions. Phytoplankton can regulate the contents of cellular complexes (i.e.,  
113 pigments and ribosomes) to acclimate to different irradiance or temperature  
114 conditions, which can further influence their relative N:P requirement (Thrane *et al.*  
115 2016, 2017). Furthermore, Galbraith and Martiny (2015) emphasized that the cellular  
116 P of phytoplankton has greater plasticity than cellular N, resulting in high  
117 phytoplankton N:P ratios in oligotrophic waterbodies. Phytoplankton may have a  
118 basic and steady requirement for N, whereas their demand for P may be much more  
119 flexible and dependent on phytoplankton growth and nutrient availability.

120       Herein, we propose that optimal supply N:P ratios would be flexible under  
121 different trophic statuses and would decline with an increase in absolute nutrient  
122 levels (Fig. 1b and c). We assumed that the response of N-fixing cyanobacterium to  
123 supply N:P ratios may differ from other phytoplankton species due to its higher  
124 tolerance to N starvation. We tested these hypotheses using previous and present  
125 experimental data on eight phytoplankton species. Most of the phytoplankton species  
126 tested in the present study, including a N-fixing cyanobacterium, yielded similar  
127 results supporting our hypothesis: trophic status is negatively related to the N:P ratio  
128 required for optimal growth.

## 129 **2. Materials and methods**

### 130 **2.1 Biological material**

131 We used three phytoplankton species: the green algae *Chlorella vulgaris* NIES-  
132 2172, the cyanobacteria *Anabaena variabilis* NIES-2093 (N-fixing cyanobacterium),  
133 and *Microcystis aeruginosa* NIES-44. All axenic stock cultures were obtained from  
134 the Microbial Culture Collection of the National Institute for Environmental Studies,  
135 Tsukuba, Japan. Stock cultures were transferred into a modified BG-11 medium,  
136 added with 0.1  $\mu\text{mol L}^{-1}$  vitamin B<sub>12</sub> and 0.1  $\mu\text{mol L}^{-1}$  biotin. All stock cultures were  
137 grown under controlled conditions with a light intensity of 15  $\mu\text{mol photons m}^{-2} \text{s}^{-1}$   
138 and a temperature of 24 °C for a two-transfer acclimation period.

### 139 **2.2 Experimental design**

140 To maximize the absolute nutrient concentration and the supply N:P ratio  
141 gradients, we set the concentrations of N and P to have 12 levels each (Table S1 and  
142 Figure S1). According to trophic state classification criteria, the nutrient levels for N  
143 and P range from oligotrophic to hypereutrophic (Schlesinger & Bernhardt 2020).  
144 Forty-eight combinations of N and P were prepared for each of the three  
145 phytoplankton species, with each level of N or P replicated four times (Fig. S1). The  
146 concentration of all other nutrients was determined based on the composition of the  
147 BG-11 medium, which reduced the risk of nutrient limitation by factors other than N  
148 and P.

149 To test whether the effects of the N:P ratio on phytoplankton growth would



150 change under different trophic statuses, we categorized the combinations of resource  
151 stoichiometries into a series of nutrient levels. Accordingly, we defined the nutrient  
152 levels of different resource stoichiometries by assigning weights to N and P. The  
153 nutrient supply level (NSL) was defined as the combined result of the absolute  
154 concentrations of N and P and expressed as  $NSL = (C_N + 16C_P) / 32$ , where  $C_N$  and  $C_P$   
155 represent the concentrations of N and P resources ( $\mu\text{mol L}^{-1}$ ), respectively. The weight  
156 allocated to P was defined as 16 times N based on the Redfield ratio (the average N:P  
157 ratio of 16:1 observed in marine phytoplankton; Redfield 1934); thus, the NSL of a  
158 nutrient resource combination with  $16 \mu\text{mol L}^{-1}$  N and  $1 \mu\text{mol l}^{-1}$  P would be  
159 calculated as 1. All N and P combinations (white dots) on decreasing diagonal lines  
160 shared the same NSL value, and the value increased across the X-Y plane (Fig. S1).  
161 This method ensured that each specific N:P ratio value could be found for any NSL.

### 162 ***2.3 Experiment execution***

163 We conducted the experiment using 48-well microplates (AGC Techno Glass Co.,  
164 Ltd., Shizuoka, Japan), with each well containing  $750 \mu\text{L}$  medium prepared based on  
165 the modified BG-11 medium described above. Prior to the experiment, exponentially  
166 growing cultures were harvested through centrifugation ( $4000 \times g$  for 8 min), washed  
167 with ultrapure water, transferred into BG-11 medium modified to be N-free ( $\text{NaNO}_3$   
168 replaced with an equimolar equivalent of NaCl, and ferric ammonium citrate  
169 substituted with ferric citrate) and P-free ( $\text{K}_2\text{HPO}_4$  replaced with an equimolar  
170 equivalent of KCl), and cultivated under the aforementioned conditions for three days

171 to reduce the effects of N and P stored in phytoplankton cells (Huang *et al.* 2014; Ren  
172 *et al.* 2017).

173 At the start of the experiment (day 0), each well was inoculated with 40  $\mu\text{L}$   
174 phytoplankton stock culture (initial optical density at 595 nm [ $\text{OD}_{595}$ ] < 0.05;  
175 background  $\text{OD}_{595}$  of the BG-11 medium was approximately 0.03–0.04). All  
176 microplates were kept in a climate-controlled room at 24 °C with a 16:8 h light:dark  
177 cycle of 15  $\mu\text{mol photons s}^{-1} \text{m}^{-2}$ . Irradiance was measured using an LI-1400 data  
178 logger (Li-Cor, Lincoln, NE, USA). All microplates were covered with a gas-  
179 permeable sealing membrane (Breathe-Easy; Sigma-Aldrich, St. Louis, MO, USA) to  
180 prevent evaporation and microbial contamination. The microplates were randomly  
181 rearranged daily to ensure comparable light conditions during the experiment. The  
182 experiments were initiated in batch cultures. After one week of cultivation, we shifted  
183 the batch cultures into semi-continuous cultures. The dilution rate was 0.15  $\text{d}^{-1}$ , which  
184 was achieved by replacing 15% of the well volume with fresh culture medium under a  
185 laminar flow cabinet every day to refresh the culture media and extend the steady-  
186 state growth phase. Each experiment was terminated when the respective culture  
187 reached the steady-state growth phase.

#### 188 ***2.4 Monitoring phytoplankton growth***

189 To determine whether the phytoplankton cultures had reached a quasi-steady  
190 state, the  $\text{OD}_{595}$  in each well was measured daily using a microplate reader (Infinite  
191 F200 PRO; Tecan Group Ltd., Männedorf, Switzerland).  $\text{OD}_{595}$  has been widely used

192 as a proxy for monitoring phytoplankton growth (Huesemann *et al.* 2009; Kapoore *et*  
193 *al.* 2019); we demonstrated that OD<sub>595</sub> is highly correlated with the cell density of the  
194 three phytoplankton species (Fig. S2a–c). However, OD measurements for  
195 phytoplankton biomass are susceptible to errors due to pigment interference during  
196 different growth phases (Griffiths *et al.* 2011). Therefore, to better evaluate the culture  
197 biomass, a colorimetric analysis was performed according to our preparatory work  
198 (Jiang & Nakano, 2021). Immediately before cell enumeration of the three  
199 phytoplankton species (day 14 for *A. variabilis*, day 16 for *M. aeruginosa*, and day 21  
200 for *C. vulgaris*), RGB (red, green, and blue) color information for the phytoplankton  
201 cultures was collected using a free mobile application called “Color-Meter”  
202 (<https://apps.apple.com/us/app/color-meter/id1512406137>; accessed on 1st December  
203 2021). The RGB color information was then converted into the HSI (hue, saturation,  
204 intensity) color space for subsequent analysis (Jiang & Nakano, 2021). The results  
205 indicated that variations in the hue of the experimental phytoplankton cultures were  
206 limited (Fig. S3a), thereby verifying the validity of the optical and colorimetric  
207 analyses. Additionally, the measurements of the phytoplankton biomass via OD<sub>595</sub> and  
208 color intensity were highly correlated (Fig. S3b–d). We used the results of the optical  
209 and colorimetric analyses to confirm that the cultures reached a quasi-steady state, as  
210 the timing varied depending on the cultivation conditions (Fig. S4). However, the  
211 steady state of the phytoplankton in some experimental units could not be maintained  
212 for an extended period due to nutrient limitation (Fig. S4); thus, it was difficult to

213 accurately and timely judge whether the cultures reached a steady state during the  
214 experiments. Therefore, the steady-state OD<sub>595</sub> was estimated as the mean of the  
215 OD<sub>595</sub> values greater than 95% of the maximum OD<sub>595</sub> during the growth period for  
216 each experimental unit. We counted the cell density during the quasi-steady state or  
217 near the peak of the growth curves with a Neubauer hemocytometer (Brand,  
218 Wertheim, Germany) under an optical microscope (Olympus BX51; Olympus, Tokyo,  
219 Japan). The steady-state phytoplankton cell density ( $C_{\text{steady-state}}$ ) was calculated as:

$$220 \quad C_{\text{steady-state}} = C_{\text{count}} \frac{\text{OD}_{595(\text{steady-state})} - \text{OD}_{595(\text{BG-11})}}{\text{OD}_{595(\text{count})} - \text{OD}_{595(\text{BG-11})}}$$

221 where OD<sub>595(count)</sub> represents the OD<sub>595</sub> of the counted subsamples, OD<sub>595(stea</sub>  
222 <sub>dy-state)</sub> represents the steady-state OD<sub>595</sub>,  $C_{\text{count}}$  represents the phytoplankton cell density  
223 counted on the sampling day, and OD<sub>595(BG-11)</sub> is the background OD<sub>595</sub> value of the  
224 BG-11 medium, which was estimated to be 0.035 using a microplate reader (Infinite  
225 F200 PRO; Tecan, Austria).

## 226 **2.5 Determining the transitions between N and P requirements**

227 Each phytoplankton species contained 48 experimental units, which were  
228 classified into several different NSLs (Fig. S1). We established relationships between  
229 the supply N:P ratio and the steady-state phytoplankton cell density for four NSLs  
230 (0.91, 1.24, 1.58, and 1.91; Figs. 2 and S5). The transitions between N and P  
231 limitation at each NSL were calculated using one-dimensional locally weighted  
232 sequential smoothing method (1D-LOESS; *loess* function in Base R) by drawing  
233 “peak-shaped” relationship curves (Fig. 2). The parameter *span*, which controls the

234 degree of smoothing in 1D-LOESS, was accepted at its default value of 0.75.

235       The 1D-LOESS method provided results for limited NSLs because it can only  
236 estimate the relationships between supply N:P ratios and phytoplankton biomass  
237 based on experimental units sharing the same NSL value (Fig. 2). To obtain a  
238 continuous relationship between the optimal N:P ratio and the NSL, we estimated the  
239 relationships between two related variables (N and P concentrations) and an outcome  
240 (phytoplankton cell density during the steady-state phase) using a two-dimensional  
241 LOESS curve with a default *span* of 0.75 (2D-LOESS; *loess* function in Base R). By  
242 fitting the available 48 experimental data points to the 2D-LOESS model, the steady-  
243 state cell density could be calculated for any possible combination of N and P  
244 resource concentrations. Using the *predict* function in Base R, the estimates for each  
245 combination of N and P concentrations were generated into a matrix and visualized  
246 through contour plots to show a smoothing relationship between the resource  
247 stoichiometry and phytoplankton biomass (Fig. 3a–c). Each value of the  
248 phytoplankton density on the 2D-LOESS contours was estimated according to pre-  
249 defined (N, P) locations ([https://stat.ethz.ch/pipermail/r-help/2007-](https://stat.ethz.ch/pipermail/r-help/2007-February/125269.html)  
250 [February/125269.html](https://stat.ethz.ch/pipermail/r-help/2007-February/125269.html), accessed on 1st December 2021).

251       The phytoplankton density at the intermediate NSLs (0.74–1.94) was calculated  
252 with an interval of 0.12 based on the estimates from the 2D-LOESS contours. For  
253 each NSL, the cell density of each supply N:P ratio was extracted at an interval of less  
254 than 0.01, generating smoothing curves that described the relationships between the

255 supply N:P ratio and phytoplankton density (Fig. S6). We sorted through all  
256 phytoplankton density estimates with different supply N:P ratios and extracted the  
257 maximum value whose N:P ratio was regarded as the most optimal for that NSL (Fig.  
258 3d–f). The analytical process for determining the optimal supply N:P ratios of  
259 different nutrient levels using 2D-LOESS is shown in Figure S7.

## 260 **2.6 Literature dataset analyses**

261 Published datasets from previous studies were compared with the results of the  
262 present study. Datasets were selected based on the four following criteria: (1)  
263 phytoplankton monocultures were cultivated under conditions with different absolute  
264 and relative N and P concentrations; (2) the combinations of the supply N and P  
265 concentrations were sufficient for calculating the optimal N:P ratios for at least two  
266 NSLs; (3) the cultures were cultivated through the steady-state phase, and the steady-  
267 state biomass was determined; and (4) N and P were the only limiting factors for  
268 phytoplankton growth during cultivation. Although studies have focused on the  
269 influence of supply N:P ratios on phytoplankton growth, the majority of the obtained  
270 datasets did not cover two or more NSLs. Nevertheless, datasets derived from Frank  
271 *et al.* (2020) and Kunikane *et al.* (1984) fulfilled the aforementioned criteria.

272 For Frank *et al.* (2020), we applied the 2D-LOESS method described above to  
273 determine the effects of the NSL on the optimal supply N:P ratios during the steady  
274 state for the same four phytoplankton species in monoculture (*Ankistrodesmus* sp.,  
275 *Chlamydomonas reinhardtii*, *Scenedesmus obliquus*, and *Staurastrum* sp.) (Fig. 4a-d)

276 and in admixture (Fig. 4e). Optimal supply N:P ratios at the NSLs from 1.7 to 4.7  
277 were estimated with an interval of 0.1, and only the NSLs resulting in a unimodal  
278 curve with a peak (the curve describes the relationship between steady-state  
279 phytoplankton biomass and the supply N:P ratios; Fig. S7) were applied to assess the  
280 impacts of the NSL on the optimal supply N:P ratio (Fig. 4f-j, Fig. S7).

281 In Kunikane *et al.* (1984), higher dilution rates led to higher available N and P  
282 concentrations in the medium during the steady-state phase, which was equivalent to  
283 the high NSLs used in the present study. We calculated the transitions between N and  
284 P requirements using smoothing spline curves in GraphPad Prism (GraphPad, San  
285 Diego, CA, USA) (Fig. 4k and l).

286 The dataset in Frank *et al.* (2020) was directly obtained from the authors, whereas  
287 the data presented in Figure 4 of Kunikane *et al.* (1984) was estimated using the open-  
288 access digitizing software Engauge Digitizer version 12.1 because we were unable to  
289 contact the authors.

### 290 **3. Results**

291 For most of the NSLs of the three phytoplankton species, the steady-state  
292 phytoplankton density followed a significant unimodal relationship with the supply  
293 N:P ratio, with the exceptions of *C. vulgaris* and *A. variabilis* cultures at the NSL of  
294 1.91 (Fig. 2). The optimal ratios estimated using 1D-LOESS generally decreased with  
295 an increased NSL (Fig. 2). 2D-LOESS predictions of the relationships between the  
296 supply N:P ratio and the NSL were obtained from all 48 experimental units rather than

297 only the experimental units having the same NSL (Fig. 3a–c), and this method  
298 generated more detailed relationships between the optimal supply N:P ratio and the  
299 NSL. The results of the 2D-LOESS models showed the same pattern as the 1D-  
300 LOESS: the optimal supply N:P ratio decreased with the increase in NSL for all three  
301 studied phytoplankton species (Fig. 3d–f).

302 The datasets obtained from the literature also supported this trend. Three of the  
303 four phytoplankton species studied by Frank *et al.* (2020) were found to have the  
304 decrease in optimal supply N:P ratio with an increasing NSL (Fig. 4f–i). *C. reinhardtii*  
305 was the only exception, as its optimal supply N:P ratios were distributed in a narrow  
306 range (mean  $\pm$  SD:  $23.9 \pm 1.2$ ; Fig. 4i). In addition, the results of the mixed culture in  
307 Frank *et al.* (2020) showed a similar trend of a decreasing optimal supply N:P ratio  
308 with NSLs (Fig. 4j). The calculated results of the data from Kunikane *et al.* (1984)  
309 indicated that the optimal N:P ratios of *S. dimorphus* decreased with the increase in  
310 dilution rate (Fig. 4l). At the steady state observed in the chemostat, the growth rate of  
311 the phytoplankton density was equal to the dilution rate. In other words,  
312 phytoplankton with high growth rates tended to require more P than N. Overall, seven  
313 out of the eight analyzed phytoplankton species exhibited a decreasing optimal supply  
314 N:P ratio with the increase in nutrient availability. This trend was achieved under  
315 different culture conditions (i.e., semi-continuous culture in the present study, batch  
316 cultures in Frank *et al.* [2020], and chemostat cultures in Kunikane *et al.* [1984]) and  
317 methods for regulating the absolute nutrient concentrations (i.e., varying input



318 nutrients in the present study and Frank *et al.* [2020], varying dilution rates in  
319 Kunikane *et al.* [1984]).

320 Although the optimal supply N:P ratio generally decreased with the increase in  
321 NSL, the downward trend was not immutable, especially for high NSLs. The decline  
322 tended to level off at high NSLs (or high dilution rates in the chemostat experiment),  
323 which was observed in half of the studied species: *C. vulgaris* and *M. aeruginosa*  
324 cultures in the present experiments (Fig. 3), *S. obliquus*, *Staurastrum* sp. and mixed  
325 cultures in Frank *et al.* (2020), and *S. dimorphus* in Kunikane *et al.* (1984) (Fig. 4).

#### 326 **4. Discussion**

327 N and P requirements for phytoplankton growth seem to be flexible among  
328 various trophic statuses, as reflected by the decrease of the optimal supply N:P ratio  
329 with the increase in NSL. The optimal supply N:P ratio was defined as the supply N:P  
330 ratio in a medium where the transition from N limitation to P limitation for  
331 phytoplankton growth occurred. We found only one exception (*C. reinhardtii*) among  
332 the eight studied species (Fig. 4d and 4i), while stable ranges of the optimal supply  
333 N:P ratio were observed in half of the other phytoplankton cultures at high NSLs.  
334 Therefore, we cannot identify whether the optimal supply N:P ratio for *C. reinhardtii*  
335 was truly stable over all NSLs, or whether the NSLs studied by Frank *et al.* (2020)  
336 were too high to cover the decreasing ranges of the optimal supply N:P ratio. Despite  
337 this exception, a significant proportion of the phytoplankton species supported the  
338 conclusion that phytoplankton has higher N requirements than P requirements at low

339 NSLs, or vice versa at high NSLs. Although we focused mainly on monocultures in  
340 the present study, it is noteworthy that mixed cultures studied in Frank *et al.* (2020)  
341 produced similar results that support our hypothesis (Fig. 4j). The trend of decreasing  
342 optimal supply N:P ratio with NSLs was unaffected by species shifts within the mixed  
343 cultures. All four species in the mixed cultures belonged to a single phylum  
344 (Chlorophyta); however, we have not yet determined whether our hypothesis is also  
345 applicable to mixed cultures comprising various taxa.

346 To the best of our knowledge, this study is the first to demonstrate that trophic  
347 status is negatively related to the relative N:P requirement for phytoplankton growth.  
348 Changes in the optimal N:P ratio at different NSLs could be explained by the growth-  
349 rate hypothesis, which states that the variation in cellular N:P ratios is largely  
350 attributed to cellular protein and rRNA contents (Elser *et al.* 2000; Sterner & Elser  
351 2002), as proteins are the largest cellular N pool, and rRNAs are the largest  
352 contributor of P to phytoplankton cells (Geider & La Roche 2002; Sterner & Elser  
353 2002). For phytoplankton cultures under the same supply N:P ratio but at different  
354 NSLs, higher NSLs (or high dilution rates in the chemostat experiment) likely  
355 increased nutrient availability and promoted phytoplankton growth, resulting in higher  
356 biomass (Fig. 2–4). Phytoplankton growth enhancement would increase the rRNA  
357 requirement, resulting in a higher requirement of P relative to N. It is also possible  
358 that the changes in the optimal N:P ratios were related to certain adaptive responses of  
359 phytoplankton to low nutrient supplies. In low P environments, phytoplankton would

360 selectively increase the synthesis of P-free compounds rather than P-containing  
361 compounds to reduce the P demand, such as by replacing phospholipids in cell  
362 membranes with sulfonated lipids (Snyder *et al.* 2009; Wurch *et al.* 2011). However,  
363 N seems to be more essential for phytoplankton photosynthesis than P. N limitation in  
364 phytoplankton can cause a substantial decline in the content of the major  
365 photosynthetic pigment, chlorophyll *a*, and increase the amount of non-photosynthetic  
366 pigments (Herrig & Falkowski 1989; Geider *et al.* 1993). However, the effects of P  
367 limitation on cellular chlorophyll *a* are relatively smaller than those of N limitation  
368 (Geider *et al.* 1998). In addition, N limitation may greatly reduce the efficiency of  
369 photosystem II and the relative abundance of Rubisco in phytoplankton cells  
370 (Falkowski *et al.* 1989; Geider *et al.* 1993), whereas P limitation moderately affects  
371 phytoplankton photosystems (Geider *et al.* 1998). Accordingly, we assumed that  
372 phytoplankton may have a steady N requirement because of its importance for  
373 photosynthesis, while P requirement may be more flexible via adaptation and  
374 acclimation responses. This assumption is consistent with the results of Galbraith and  
375 Martiny (2015), who found that the cellular abundance of N in phytoplankton tends to  
376 be less plastic than the P content. Phytoplankton under dual N and P limitation,  
377 therefore, would show a higher requirement for N than P.

378       The decreasing curve of the optimal N:P ratio tended to level off with increasing  
379 NSL, as observed in half of the studied phytoplankton species (Figs. 3 and 4). For  
380 datasets derived from experiments with a factorial design (the present study and Frank

381 *et al.* [2020]), high NSLs were only studied with limited experimental units, and the  
382 supply N:P ratios of these units were distributed in a narrow range. As shown in  
383 Figure 2, the peaks of the unimodal curves became indistinct at high NSLs, and the  
384 optimal supply N:P ratios for *C. vulgaris* and *A. variabilis* at the NSL of 1.91 (molar  
385 supply N:P ratios distributed from 7.71 to 33.29) could not be identified using 1D-  
386 LOESS method. Hence, the disappearance of the decreasing trend may be partly  
387 explained by the factorial design used in the present study and by Frank *et al.* (2020).  
388 The data of Kunikane *et al.* (1984) showed similar results, as the optimal N:P ratio  
389 became stable at high absolute NSLs (Fig. 41); however, this trend could not be  
390 explained by the same reason because NSLs were regulated by dilution rates instead  
391 of nutrient input. Thus, stable optimal N:P ratios at high NSLs may not be a  
392 coincidence. Stable optimal N:P ratios at high NSLs may result from the decrease in  
393 nutrient affinity alongside the increase in absolute nutrient concentrations (Smith *et*  
394 *al.* 2009; Bonachela *et al.* 2011). Phytoplankton cells can increase the number of  
395 surface uptake sites (proteins that incorporate nutrients from the cell membrane into  
396 the cytoplasm) to increase the encounter with nutrients in low-nutrient waterbodies  
397 (Smith *et al.* 2009; Bonachela *et al.* 2011), leading to a high nutrient affinity for  
398 phytoplankton cells. With the increase in nutrient availability, phytoplankton growth  
399 is no longer limited by extracellular nutrients, and the nutrient uptake rates are thus  
400 controlled by intracellular enzymes that assimilate the encountered nutrients (Smith *et*  
401 *al.* 2009). Therefore, we can find explicitly decreasing curves of optimal N:P ratios

402 under low NSLs due to the high nutrient affinity in this phase, and the curves become  
403 stable at high NSLs because of the decrease in nutrient affinity (Fig. 5). For high  
404 NSLs, the optimal supply N:P ratios can be calculated using the 2D-LOESS method  
405 (Fig. 3), but cannot always be estimated using 1D-LOESS method (Fig. 2). The  
406 optimal N:P ratios at high NSLs derived from the 2D-LOESS method were calculated  
407 using experimental units of both high NSLs and low NSLs. So, the values calculated  
408 on the smoothing curves of high NSLs could be regarded as an inertial extension of  
409 values estimated at low NSLs. Thus, although the optimal N:P ratios at high NSLs  
410 could be calculated mathematically, the ecological significance of the calculated N:P  
411 ratios would be negligible (Fig. 5).

412       The cyanobacterium *A. variabilis* is capable of nitrogen fixation (Thiel *et al.*  
413 2014), which is thought to have the potential to offset the decline in resource N  
414 supply. The results indicate that the optimal supply N:P ratios for *A. variabilis* cultures  
415 at low NSLs are much higher than those at high NSLs (Fig. 2b and 3d). In other  
416 words, nitrogen fixation in *A. variabilis* cells did not offset the decline in the N  
417 supply, which supports the idea that, although nitrogen fixation could stimulate  
418 cyanobacterial growth, cyanobacterial N fixers do not fully compensate for N  
419 deficiency (Lewis Jr & Wurtsbaugh 2008; Scott & McCarthy 2010).

420       Experimental setups and culture systems varied between the experiment in the  
421 present study and those of previous studies from which datasets were used in the  
422 present study (Kunikane *et al.* 1984; Frank *et al.* 2020). NSLs calculated from batch

423 cultures in Frank *et al.* (2020) were almost 2.5-fold higher than NSLs calculated using  
424 data derived from the present semi-continuous cultures in the present study (Figs. 3  
425 and 4) because the initial nutrient level of the batch cultures was higher than that of  
426 the semi-continuous cultures. Additionally, both values and changing ranges of  
427 optimal supply N:P ratios calculated from the present semi-continuous cultures were  
428 lower and narrower than those in previous studies (Kunikane *et al.* 1984; Frank *et al.*  
429 2020), which could be attributed to the differences in experimental setups and  
430 phytoplankton taxa among the experiments. Additionally, light intensity applied in  
431 Frank *et al.* (2020) ( $40.45 \pm 15.00 \mu\text{mol photons m}^2 \text{ s}^{-1}$ ) was much higher than that in  
432 our study ( $15 \mu\text{mol photons m}^2 \text{ s}^{-1}$ ), which could explain the broader optimal supply  
433 N:P ratio ranges in Frank *et al.* (2020).

## 434 **5. Conclusions**

435 The response curves depicting the relationships between the optimal supply N:P  
436 ratio and trophic status varied among the eight tested phytoplankton species, but seven  
437 of them showed similar declining trends. Our results support the idea that the transition  
438 from N requirements to P requirements is not a definite boundary, but it varies  
439 depending on trophic status, with lower nutrient supply leading to higher N  
440 requirements than P requirements (Fig. 5). The N vs. P limitation for controlling  
441 phytoplankton growth has been discussed for decades, but it still remains an open  
442 question (Schindler *et al.* 2008; Conley *et al.* 2009; Xu *et al.* 2010; Paerl *et al.* 2016).  
443 The present study assumed that neither N nor P was superior in controlling

444 phytoplankton growth. P was considered to have high priority in conditions with  
445 sufficient N and P supplies (i.e., phytoplankton blooms in eutrophic waterbodies),  
446 which is consistent with studies showing that P is more effective in controlling  
447 eutrophication than N (Carpenter 2008; Schindler *et al.* 2008). In contrast, we suggest  
448 that the importance of N to phytoplankton productivity is greater in environments with  
449 a low nutrient supply (i.e., in oligotrophic waterbodies). Generally, our results could be  
450 instructive for the control of phytoplankton biomass and eutrophication mitigation in  
451 aquatic ecosystems.

#### 452 **Acknowledgements**

453 The authors thank Dr. Yukiko Goda for assistance with the experimental setup and Dr.  
454 Koichi Ito for valuable comments on statistics. Further, the authors thank Maren  
455 Striebel and Michael Danger for valuable comments on the manuscript. This work was  
456 partly supported by KAKENHI, Grants-in-Aid for Scientific Research, grant number  
457 19H03302 and 21J15473 from the Japan Society for the Promotion of Science.

458

#### 459 **References**

460 Abell, J.M., Özkundakci, D. & Hamilton, D.P. (2010). Nitrogen and Phosphorus  
461 Limitation of Phytoplankton Growth in New Zealand Lakes: Implications for  
462 Eutrophication Control. *Ecosystems*, 13, 966-977.

463

464 Bonachela, J.A., Raghieb, M. & Levin, S.A. (2011). Dynamic model of flexible

465 phytoplankton nutrient uptake. *Proceedings of the National Academy of*  
466 *Sciences*, 108, 20633-20638.

467

468 Budy, P., Luecke, C. & Wurtsbaugh, W.A. (1998). Adding Nutrients to Enhance the  
469 Growth of Endangered Sockeye Salmon: Trophic Transfer in an Oligotrophic  
470 Lake. *Transactions of the American Fisheries Society*, 127, 19-34.

471

472 Carpenter, S.R. (2008). Phosphorus control is critical to mitigating eutrophication.  
473 *Proceedings of the National Academy of Sciences*, 105, 11039-11040.

474

475 Chaffin, J.D., Bridgeman, T.B., & Bade, D.L. (2013). Nitrogen Constrains the Growth  
476 of Late Summer Cyanobacterial Blooms in Lake Erie. *Advances in*  
477 *Microbiology*, 3, 16-26

478

479 Conley, D.J., Paerl, H.W., Howarth, R.W., Boesch, D.F., Seitzinger, S.P., Havens, K.E.  
480 *et al.* (2009). Controlling Eutrophication: Nitrogen and Phosphorus. *Science*,  
481 323, 1014.

482

483 Downing, J.A. & McCauley, E. (1992). The nitrogen : phosphorus relationship in lakes.  
484 *Limnology and Oceanography*, 37, 936-945.

485



486 Elser, J.J., Bracken, M.E.S., Cleland, E.E., Gruner, D.S., Harpole, W.S., Hillebrand, H.  
487 *et al.* (2007). Global analysis of nitrogen and phosphorus limitation of primary  
488 producers in freshwater, marine and terrestrial ecosystems. *Ecology Letters*, 10,  
489 1135-1142.

490

491 Elser, J.J., Sterner, R.W., Gorokhova, E., Fagan, W.F., Markow, T.A., Cotner, J.B. *et al.*  
492 (2000). Biological stoichiometry from genes to ecosystems. *Ecology Letters*, 3,  
493 540-550.

494

495 Falkowski, P.G., Sukenik, A. & Herzig, R. (1989). Nitrogen limitation in *Isochrysis*  
496 *galbana* (Haptophyceae). II. Relative abundance of chloroplast proteins.  
497 *Journal of Phycology*, 25, 471-478.

498

499 Frank, F., Danger, M., Hillebrand, H. & Striebel, M. (2020). Stoichiometric constraints  
500 on phytoplankton resource use efficiency in monocultures and mixtures.  
501 *Limnology and Oceanography*, 65, 1734-1746.

502

503 Galbraith, E.D. & Martiny, A.C. (2015). A simple nutrient-dependence mechanism for  
504 predicting the stoichiometry of marine ecosystems. *Proceedings of the National*  
505 *Academy of Sciences*, 112, 8199-8204.

506

507 Geider, R. & La Roche, J. (2002). Redfield revisited: variability of C:N:P in marine  
508 microalgae and its biochemical basis. *European Journal of Phycology*, 37, 1-17.  
509

510 Geider, R., Macintyre, Graziano, L. & McKay, R.M. (1998). Responses of the  
511 photosynthetic apparatus of *Dunaliella tertiolecta* (Chlorophyceae) to nitrogen  
512 and phosphorus limitation. *European Journal of Phycology*, 33, 315-332.  
513

514 Geider, R.J., La Roche, J., Greene, R.M. & Olaizola, M. (1993). Response of the  
515 photosynthetic apparatus of *Phaeodactylum tricornutum* (Bacillariophyceae) to  
516 nitrate, phosphate, or iron starvation. *Journal of Phycology*, 29, 755-766.  
517

518 Griffiths, M.J., Garcin, C., van Hille, R.P. & Harrison, S.T.L. (2011). Interference by  
519 pigment in the estimation of microalgal biomass concentration by optical  
520 density. *Journal of Microbiological Methods*, 85, 119-123.  
521

522 Herrig, R. & Falkowski, P.G. (1989). Nitrogen limitation in *Isochrysis galbana*  
523 (Haptophyceae). I. Photosynthetic energy conversion and growth efficiencies.  
524 *Journal of Phycology*, 25, 462-471.  
525

526 Hillebrand, H., Steinert, G., Boersma, M., Malzahn, A., Meunier, C.L., Plum, C. *et al.*  
527 (2013). Goldman revisited: Faster growing phytoplankton has lower N:P and

528 lower stoichiometric flexibility. *Limnology and Oceanography*. 58, 2076–2088.

529

530 Huang, W., Bi, Y. & Hu, Z. (2014). Effects of Fertilizer-Urea on Growth, Photosynthetic  
531 Activity and Microcystins Production of *Microcystis aeruginosa* Isolated from  
532 Dianchi Lake. *Bulletin of Environmental Contamination and Toxicology*, 92,  
533 514-519.

534

535 Huesemann, M.H., Hausmann, T.S., Bartha, R., Aksoy, M., Weissman, J.C. &  
536 Benemann, J.R. (2009). Biomass Productivities in Wild Type and Pigment  
537 Mutant of *Cyclotella* sp. (Diatom). *Applied Biochemistry and Biotechnology*,  
538 157, 507-526.

539

540 Jiang, M. & Nakano, S. (2021). Application of image analysis for algal biomass  
541 quantification: a low-cost and non-destructive method based on HSI color space.  
542 *Journal of Applied Phycology*, 33, 3709–3717.

543

544 Klausmeier, C. A., Litchman, E. & Levin, S.A. (2004). Phytoplankton growth and  
545 stoichiometry under multiple nutrient limitation. *Limnology and Oceanography*.  
546 49, 1463–1470.

547

548 Kapoore, R.V., Huete-Ortega, M., Day, J.G., Okurowska, K., Slocombe, S.P., Stanley,

549 M.S. *et al.* (2019). Effects of cryopreservation on viability and functional  
550 stability of an industrially relevant alga. *Scientific Reports*, 9, 2093.

551

552 Kelly, P.T., Taylor, J.M., Andersen, I.M., Stovall, J. and Scott, J.T. (2021). Highest  
553 primary production achieved at high nitrogen levels despite strong  
554 stoichiometric imbalances with phosphorus in hypereutrophic experimental  
555 systems. *Limnology and Oceanography*. 66, 4375-4390.

556

557 Kunikane, S., Kaneko, M. & Maehara, R. (1984). Growth and nutrient uptake of green  
558 alga, *Scenedesmus dimorphus*, under a wide range of nitrogen/phosphorus  
559 ratio—I. Experimental study. *Water Research*, 18, 1299-1311.

560

561 Lewis Jr, W.M. & Wurtsbaugh, W.A. (2008). Control of Lacustrine Phytoplankton by  
562 Nutrients: Erosion of the Phosphorus Paradigm. *International Review of*  
563 *Hydrobiology*, 93, 446-465.

564

565 Lewis, W.M., Wurtsbaugh, W.A. & Paerl, H.W. (2011). Rationale for Control of  
566 Anthropogenic Nitrogen and Phosphorus to Reduce Eutrophication of Inland  
567 Waters. *Environmental Science & Technology*, 45, 10300-10305.

568

569 Liu, J. & Vyverman, W. (2015). Differences in nutrient uptake capacity of the benthic

570 filamentous algae *Cladophora* sp., *Klebsormidium* sp. and *Pseudanabaena* sp.  
571 under varying N/P conditions. *Bioresource Technology*, 179, 234-242.  
572

573 Loladze, I. & Elser, J.J. (2011). The origins of the Redfield nitrogen-to-phosphorus ratio  
574 are in a homeostatic protein-to-rRNA ratio. *Ecology Letters*, 14, 244-250.  
575

576 Paerl, H.W. (2009). Controlling Eutrophication along the Freshwater–Marine  
577 Continuum: Dual Nutrient (N and P) Reductions are Essential. *Estuaries and  
578 Coasts*, 32, 593-601.  
579

580 Paerl, H.W., Scott, J.T., McCarthy, M.J., Newell, S.E., Gardner, W.S., Havens, K.E. *et*  
581 *al.* (2016). It Takes Two to Tango: When and Where Dual Nutrient (N & P)  
582 Reductions Are Needed to Protect Lakes and Downstream Ecosystems.  
583 *Environmental Science & Technology*, 50, 10805-10813.  
584

585 Paerl, H.W., Xu, H., McCarthy, M.J., Zhu, G., Qin, B., Li, Y. *et al.* (2011). Controlling  
586 harmful cyanobacterial blooms in a hyper-eutrophic lake (Lake Taihu, China):  
587 The need for a dual nutrient (N & P) management strategy. *Water Research*, 45,  
588 1973-1983.  
589

590 Rasdi, N.W. & Qin, J.G. (2015). Effect of N:P ratio on growth and chemical

591 composition of *Nannochloropsis oculata* and *Tisochrysis lutea*. *Journal of*  
592 *Applied Phycology*, 27, 2221-2230.

593

594 Redfield, A. (1934). On the proportions of organic derivatives in sea water and their  
595 relation to the composition of plankton. In Daniel, R.J. (ed James Johnstone  
596 Memorial Volume). University Press of Liverpool, 177–192.

597

598 Reeder, B.C. (2017). Primary productivity limitations in relatively low alkalinity, high  
599 phosphorus, oligotrophic Kentucky reservoirs. *Ecological Engineering*, 108,  
600 477-481.

601

602 Ren, L., Wang, P., Wang, C., Chen, J., Hou, J. & Qian, J. (2017). Algal growth and  
603 utilization of phosphorus studied by combined mono-culture and co-culture  
604 experiments. *Environmental Pollution*, 220, 274-285.

605

606 Saito, M.A., Goepfert, T.J. & Ritt, J.T. (2008). Some thoughts on the concept of  
607 colimitation: Three definitions and the importance of bioavailability. *Limnology*  
608 *and Oceanography*, 53, 276-290.

609

610 Schindler, D.W., Hecky, R.E., Findlay, D.L., Stainton, M.P., Parker, B.R., Paterson, M.J.  
611 *et al.* (2008). Eutrophication of lakes cannot be controlled by reducing nitrogen

612 input: Results of a 37-year whole-ecosystem experiment. *Proceedings of the*  
613 *National Academy of Sciences*, 105, 11254-11258.

614

615 Schlesinger, W.H. & Bernhardt, E.S. (2020). Chapter 8 - Inland Waters. In:  
616 *Biogeochemistry (Fourth Edition)* (eds. Schlesinger, WH & Bernhardt, ES).  
617 Academic Press, pp. 293-360.

618

619 Scott, J.T. & McCarthy, M.J. (2010). Nitrogen fixation may not balance the nitrogen  
620 pool in lakes over timescales relevant to eutrophication management.  
621 *Limnology and Oceanography*, 55, 1265-1270.

622

623 Smith, S.L., Yamanaka, Y., Pahlow, M. & Oschlies, A. (2009). Optimal uptake kinetics:  
624 physiological acclimation explains the pattern of nitrate uptake by  
625 phytoplankton in the ocean. *Marine Ecology Progress Series*, 384, 1-12.

626

627 Smith, V.H. (1990). Nitrogen, phosphorus, and nitrogen fixation in lacustrine and  
628 estuarine ecosystems. *Limnology and Oceanography*, 35, 1852-1859.

629

630 Snyder, D.S., Brahamsha, B., Azadi, P. & Palenik, B. (2009). Structure of  
631 Compositionally Simple Lipopolysaccharide from Marine Synechococcus.  
632 *Journal of Bacteriology*, 191, 5499-5509.

633

634 Sperfeld, E., Martin-Creuzburg, D. & Wacker, A. (2012). Multiple resource limitation  
635 theory applied to herbivorous consumers: Liebig's minimum rule vs. interactive  
636 co-limitation. *Ecology Letters*, 15, 142-150.

637

638 Sperfeld, E., Raubenheimer, D. & Wacker, A. (2016). Bridging factorial and gradient  
639 concepts of resource co-limitation: towards a general framework applied to  
640 consumers. *Ecology Letters*, 19, 201-215.

641

642 Sterner, R.W. & Elser, J.J. (2002). How to Build an Animal: The Stoichiometry of  
643 Metazoans. In: *Ecological Stoichiometry: Biology of Elements from Molecules*  
644 *to the Biosphere*. Princeton University Press, pp. 135-178.

645

646 Thiel, T., Pratte, B.S., Zhong, J., Goodwin, L., Copeland, A., Lucas, S. *et al.* (2014).  
647 Complete genome sequence of *Anabaena variabilis* ATCC 29413. *Standards in*  
648 *Genomic Sciences*, 9, 562-573.

649

650 Thrane, J.-E., Hessen, D.O. & Andersen, T. (2016). The impact of irradiance on optimal  
651 and cellular nitrogen to phosphorus ratios in phytoplankton. *Ecology Letters*, 19,  
652 880-888.

653



654 Thrane, J.-E., Hessen, D.O. & Andersen, T. (2017). Plasticity in algal stoichiometry:  
655 Experimental evidence of a temperature-induced shift in optimal supply N:P  
656 ratio. *Limnology and Oceanography*, 62, 1346-1354.

657

658 Tilman, D. (1980). Resources: A Graphical-Mechanistic Approach to Competition and  
659 Predation. *The American Naturalist*, 116, 362-393.

660

661 Wurch, L.L., Bertrand, E.M., Saito, M.A., Van Mooy, B.A.S. & Dyhrman, S.T. (2011).  
662 Proteome Changes Driven by Phosphorus Deficiency and Recovery in the  
663 Brown Tide-Forming Alga *Aureococcus anophagefferens*. *PloS one*, 6, e28949.

664

665 Xu, H., Paerl, H.W., Qin, B., Zhu, G. & Gao, G. (2010). Nitrogen and phosphorus  
666 inputs control phytoplankton growth in eutrophic Lake Taihu, China. *Limnology  
667 and Oceanography*, 55, 420-432.

668

669 Yan, Z., Han, W., Peñuelas, J., Sardans, J., Elser, J.J., Du, E. *et al.* (2016). Phosphorus  
670 accumulates faster than nitrogen globally in freshwater ecosystems under  
671 anthropogenic impacts. *Ecology Letters*, 19, 1237–1246.

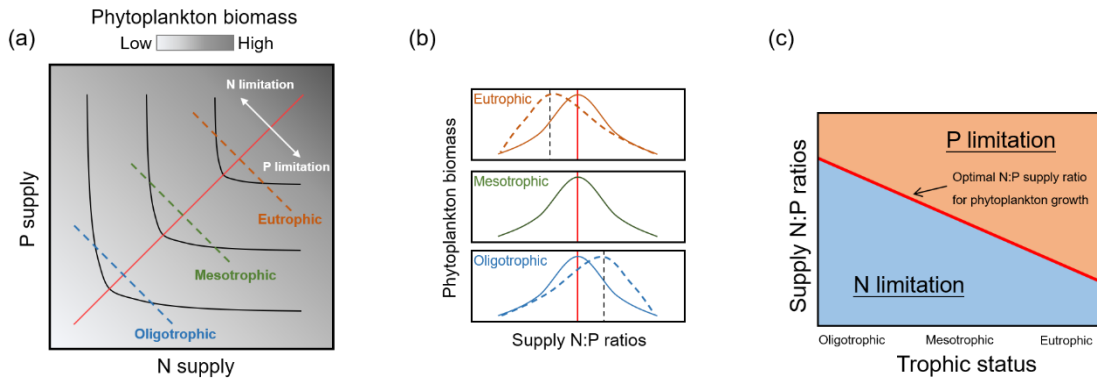
672

673 Yang, Y., Pan, J., Han, B.-P. & Naselli-Flores, L. (2020). The effects of absolute and  
674 relative nutrient concentrations (N/P) on phytoplankton in a subtropical

675 reservoir. *Ecological Indicators*, 115, 106466.

676

677



679

680 **Figure 1** Hypothesis of the experiment. (a) Hypothetical response of phytoplankton  
 681 growth under simultaneous co-limitation of nitrogen (N) and phosphorus (P) (Saito *et*  
 682 *al.* 2008; Sperfeld *et al.* 2012; Sperfeld *et al.* 2016). Resource-dependent growth  
 683 isoclines (black lines) indicate equal growth at varying resource availabilities. Colored  
 684 dash lines represent the trophic statuses. The red line indicates the optimal supply N:P  
 685 ratio. (b) Unimodal relationship between supply N:P ratios and phytoplankton biomass  
 686 under different trophic statuses. Solid colored curves represent the hypotheses of  
 687 previous studies that the position of the peaks are fixed. Dashed colored curves  
 688 represent the hypothesis of the present study that the peaks will shift with trophic status  
 689 (i.e., that higher trophic statuses have lower optimal supply N:P ratios, and lower  
 690 trophic statuses have higher ratios). (c) The predicted development of the optimal N:P  
 691 ratios, which have a negative relationship with trophic status. Phytoplankton tend to be  
 692 more P-limited than N-limited at high trophic statuses, and vice versa at low trophic  
 693 statuses.

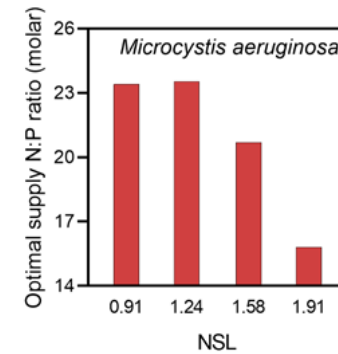
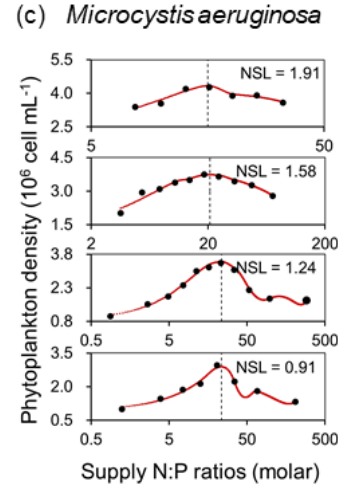
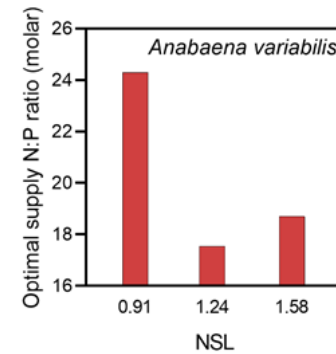
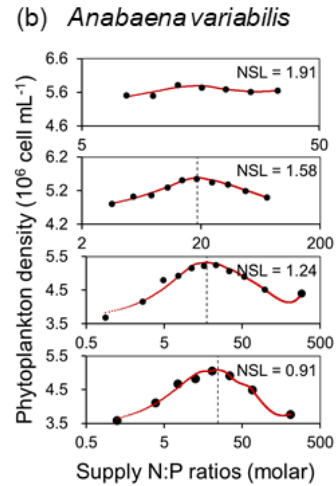
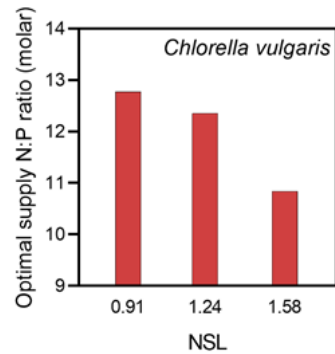
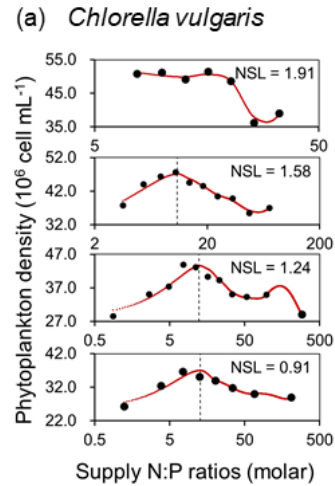


**Figure 2** Analytical results of the one-dimensional locally weighted sequential smoothing method (1D-LOESS). Response curves of steady-state phytoplankton biomass (cell density) of (a) *C. vulgaris*, (b) *A. variabilis*, and (c) *M. aeruginosa* to the supply N:P ratios under four NSLs (0.91, 1.24, 1.58, and 1.91). Dashed lines represent the position of the optimal supply N:P ratios calculated using 1D-LOESS fits. The bar graphs summarize the calculated optimal supply N:P ratios under each NSL for the corresponding phytoplankton species.

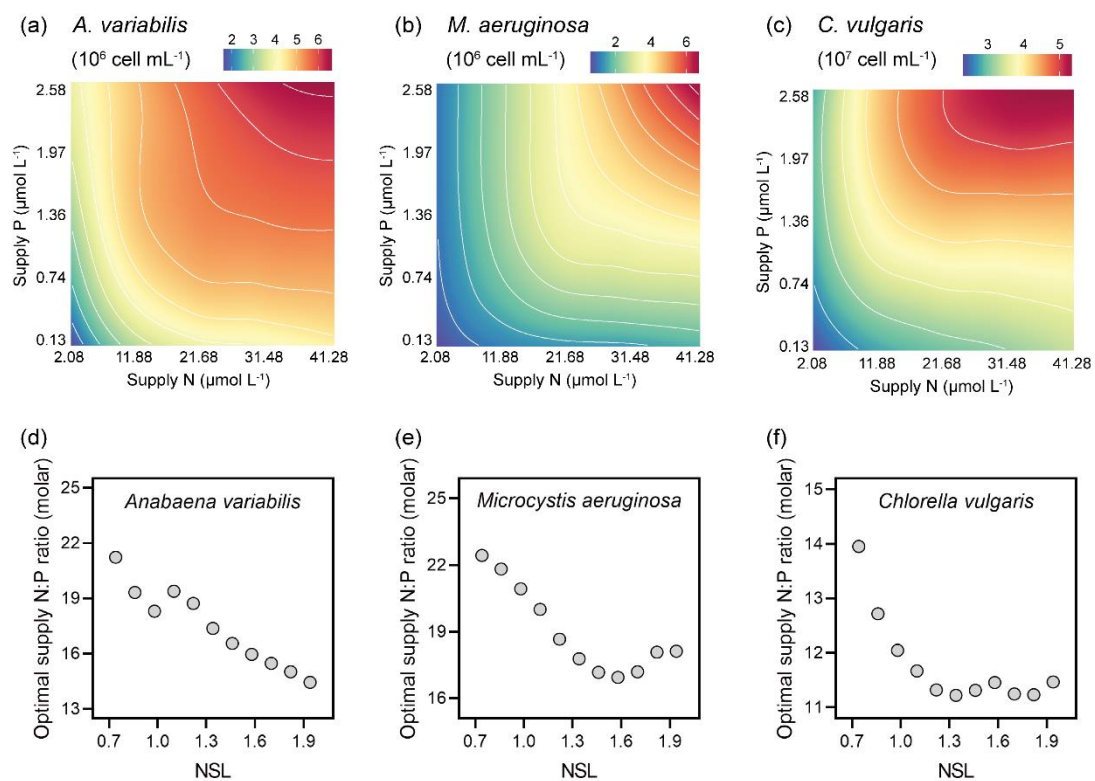


**Figure 3** 2D-LOESS response surface contours of the effects of nitrogen (N) and phosphorus (P) on the steady-state phytoplankton biomass of (a) *C. vulgaris*, (b) *A. variabilis*, and (c) *M. aeruginosa*. (d–f) Summary of the relationships between the optimal supply N:P ratios and the NSLs for the three phytoplankton species. Results were derived from the 2D-LOESS response surface contours.

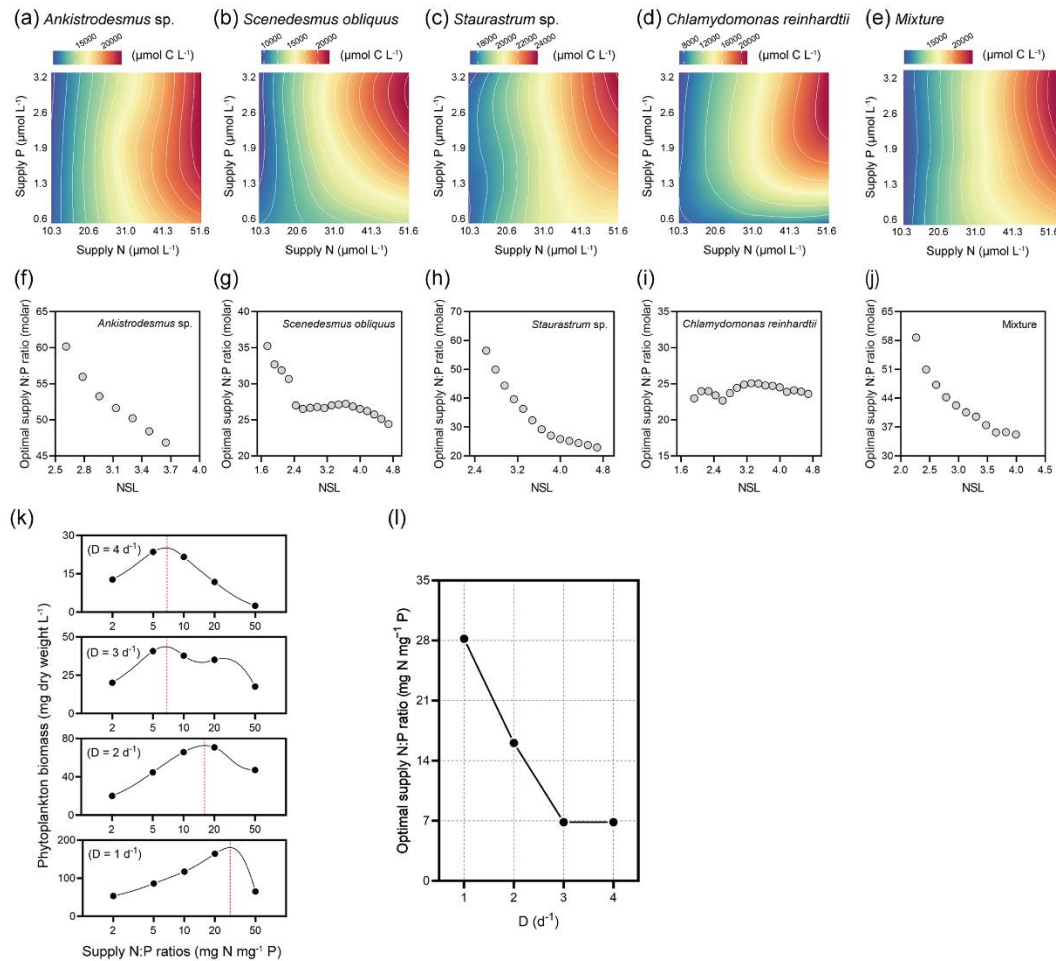


**Figure 4** Literature data review. 2D-LOESS response surface contours were applied to the data of Frank *et al.* (2020) to assess the effects of N and P on the steady-state phytoplankton biomass of (a) *Ankistrodesmus* sp., (b) *Scenedesmus obliquus*, (c) *Staurastrum* sp., (d) *Chlamydomonas reinhardtii*, and (e) mixed cultures. Relationships between the optimal supply N:P ratios and NSLs were determined for (f) *Ankistrodesmus* sp., (g) *S. obliquus*, (h) *Staurastrum* sp., (i) *C. reinhardtii*, and (j) mixed cultures, which were derived from the corresponding 2D-LOESS response surface contours (a–e). With the data of Kunikane *et al.* (1984), we examined the (k) response curves of the steady-state biomass of *Scenedesmus dimorphus* to the supply N:P ratios under four dilution rates ( $D$ ,  $\text{d}^{-1}$ ), and (l) the change in the optimal supply N:P ratios at different levels of  $D$ .

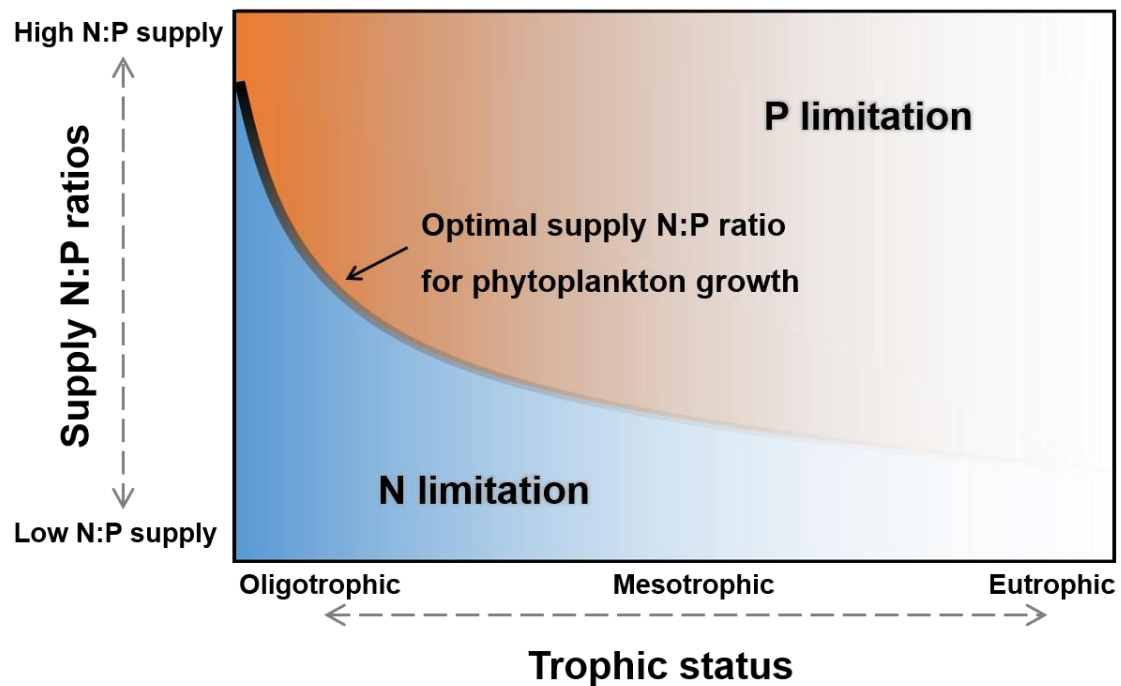


**Figure 5** Schematic of the effects of trophic status on the relative N:P limitations for phytoplankton growth. The threshold between N limitation (blue area) and P limitation (orange area) is determined by the curve of the optimal supply N:P ratio. The curve of the optimal supply N:P ratio decreases with the rise of the trophic status. The decreasing curve is steep during low trophic phases and becomes shallow at high trophic phases. Additionally, the threshold between the N and P limitations for phytoplankton may become indistinct at high trophic phases due to the decreased affinity for nutrients.